

High energy electron-beam irradiation effects in Si-SiO_x structures

D Nesheva^{1*}, V Dzhurkov¹, M Šćepanović², I Bineva¹, E Manolov¹, S Kaschieva¹, N Nedev³, S N Dmitriev⁴ and Z V Popović²

¹ Institute of Solid State Physics, Bulgarian Academy of Sciences, 72 Tzarigradsko Chaussee Blvd, 1784 Sofia, Bulgaria

² Center for Solid State Physics and New Materials, Institute of Physics, University of Belgrade, Pregrevica 118, Belgrade 11080, Serbia

³ Institute of Engineering, Autonomous University of Baja California, Benito Juarez Blvd. s/n, C.P. 21280, Mexicali, B.C., Mexico

⁴ Joint Institute for Nuclear Research, Flerov Laboratory of Nuclear Reactions, Dubna, Moscow region 141980, Russia

E-mail: nesheva@issp.bas.bg

Abstract. Homogeneous SiO_x films ($x=1.3$, 200 nm and 1000 nm thick) and composite a-Si-SiO_y films ($y \sim 1.80$) containing amorphous Si nanoparticles have been prepared on crystalline (c-Si) substrate. A part of the films was irradiated at temperature below 50 °C by 20 MeV electrons with two different fluences (7.2×10^{14} and 1.44×10^{15} el.cm⁻²). Atomic force microscopy (AFM), Raman spectroscopy and capacitance (conductance) - voltage ($C(G)$ - V) measurements on Al/c-Si/SiO_x/Al or Al/c-Si/(a-Si-SiO_y)/Al structures were used to get information about the irradiation induced changes in the surface morphology, the phase composition in the film bulk and at the Si-SiO_x interface. The AFM results show that the electron irradiation decreases the film surface roughness of the films annealed at 250 °C. The Raman scattering data imply appearance of amorphous silicon phase and some structural changes in the oxide matrix of the homogeneous SiO_x films. In the composite films electron beam stimulated decrease of the defects at the a-Si/SiO_y interface has been assumed. The initial $C(G)$ - V results speak about electron induced formation of electrically active defects in the SiO_y matrix of the composite films.

1. Introduction

Electron or ion irradiation of solids normally causes formation of atomic defects in a solid state target and spoils its properties. It may result in irradiation-induced amorphization, recrystallization and annealing. The radiation induced changes of electrical properties of solid-state materials and devices may cause an electronic device or system to fail. Therefore during the last few decades there was significant activity to explore such alterations in various types of semiconductor devices, in particular in those based on metal-oxide-silicon (MOS) structures [1, 2]. The basic radiation problem in a MOS transistor is appearance of radiation-induced trapped charge, built up in the gate oxide and traps right at the Si/SiO₂ interface, which causes a shift in the threshold voltage. If this shift is large enough, the device cannot be turned off, even at zero volts applied. The interface traps are localized states with energy levels in the Si band-gap and their occupancy is determined by the applied voltage, giving rise to a voltage-dependent threshold shift [1, 2].



Irradiation may also cause formation of amorphous nanosized domains and nanocrystals with either the original composition and crystal structure or new nanophases formed by decomposition of the target material. [3, 4]. Evolution of atom displacement cascades, radiation-induced defect generation and accumulation, as well as radiation-induced segregation are regarded as mechanisms involved in the process of nanophase formation. An area of research activity in this field is formation of nanosized Si particles in silicon oxide films which are prospective for development of new functional materials and devices suitable for usage in intense radiation fields in spacecraft, medicine, nuclear power plants, etc.

Electron irradiation has been carried out in high voltage transmission electron microscopes. Formation of amorphous or crystalline Si nanoparticles in a silicon oxide thin film matrix has been reported [5-7]. Irradiation with a high intensity convergent 100 or 200 keV electron beam at very high fluences (10^7 - 10^9 C \times m $^{-2}$ i.e. 10^{22} - 10^{24} el \times cm $^{-2}$) has been performed under ultrahigh vacuum conditions and ambient [6, 7] or high temperature [5]. It has been assumed that valence electron ionization is the key factor for the transformation from SiO $_2$ to amorphous Si while beam heating and knock-on atom displacement are responsible for the transformation from amorphous to crystalline Si [7].

To the best of our knowledge, the information on the effect of high energy electrons (> 10 MeV) on the processes of the nanoparticle growth in silicon oxide matrices and the crystallization/amorphization of Si nanoparticles is very limited [3]. Our previous investigations on c-Si/SiO $_2$ (20 nm thick) structures irradiated at ambient temperature in air by 20 MeV electrons with a fluence of 1.2×10^{15} el \times cm $^{-2}$ have shown silicon nanoparticle formation [3, 8, 9]. On the other hand the 20 MeV electron irradiation of 200 and 1000 nm thick homogeneous SiO $_x$ ($x = 1.3$) layers on c-Si substrate with a fluence of 2.4×10^{14} el \times cm $^{-2}$ have not given rise to Si nanoparticle formation in the SiO $_x$ layers [10].

In this work, the effect of 20 MeV electron irradiation with higher fluences (7.2×10^{14} el \times cm $^{-2}$ and 1.44×10^{15} el \times cm $^{-2}$) on the surface morphology, the phase separation process and the charge trapping in two types of structures, c-Si/SiO $_x$ and c-Si/(a-Si-SiO $_y$), is investigated.

2. Experimental details

2.1 Sample preparation

Silicon suboxide SiO $_x$ layers with an initial composition of $x = 1.3$ [11] and thickness of 200 and 1000 nm were prepared by thermal evaporation of SiO at a vacuum of 1×10^{-3} Pa on p or n-type (100) c-Si substrates ((7.2-10) and (4-6) $\Omega \times$ cm for p or n-type Si, respectively) maintained at room temperature. Prior to film deposition the silicon wafers were cleaned chemically using a standard procedure for the microelectronics industry. The deposition rate and film thickness were monitored by a calibrated quartz microbalance system. All as-deposited layers were annealed at 250 $^{\circ}$ C for 30 min in an Ar atmosphere to keep them stable at ambient conditions. This annealing procedure does not give rise to formation of pure silicon phase [11]. In a part of the samples, amorphous Si nanoparticles were grown in the SiO $_x$ layers by an additional furnace annealing at 700 $^{\circ}$ C in argon for 60 min, thus producing a-Si-SiO $_y$ composite layers [12]. The annealing process was used not only for growing of silicon nanoparticles but also to form simultaneously a dielectric layer with tunneling thickness at the interface with the silicon wafer.

Both kinds of structures, c-Si/SiO $_x$ ($x = 1.3$) and c-Si/(a-Si-SiO $_y$) ($y \sim 1.8$ [13]), were irradiated with 20 MeV electrons with two different fluences, $F_1 = 7.2 \times 10^{14}$ el \times cm $^{-2}$ and $F_2 = 1.44 \times 10^{15}$ el \times cm $^{-2}$. The irradiation was carried out in Microtron MT-25 in FLNR, Joint Institute for Nuclear Research, Dubna. The beam current was about $I_e = 5$ μ A. The sample temperature was controlled during the entire irradiation process and kept close to room temperature.

2.2 Sample characterization

Atomic force microscopy (AFM) technique was used to study the surface morphology of the films.

The measurements were carried out in tapping mode using a Multimode V microscope (Bruker, Santa Barbara, CA). The image resolution was 512 lines per scan direction for all measurements and the scan rate was 1 Hz. Aluminum coated silicon cantilevers TAP150-Al-G (Budget Sensors, Bulgaria) with a nominal resonance frequency of 150 kHz and a typical force constant of 5 N/m were used; the tip radius is less than 10 nm. All images were just flattened and no further processing was carried out. Roughness measurements were performed using Nanoscope 7.30 programme.

Stokes micro-Raman scattering measurements were performed in the backscattering geometry by a Jobin-Yvon T64000 triple spectrometer system, equipped with a confocal microscope and a nitrogen-cooled CCD detector. Spectra were collected by using the 532 nm (2.33 eV) line of a mixed Ar^+/Kr^+ ion laser at room temperature in the air. A low output laser power (≤ 5 mW) was used to avoid local sample heating and subsequent phase separation.

High frequency capacitance-voltage (C - V) and parallel conductance-voltage (G - V) measurements at 1 MHz were carried out to study the electron irradiation induced changes of the interface and oxide defects in MOS capacitors with a-Si-SiO_y composite layers. The MOS capacitors were prepared by depositing thin Al layers as top (gate) and back contacts. The top Al metallization was carried out through a mask and MOS capacitors with area of $\sim 2 \times 10^{-3} \text{ cm}^2$ were formed. The structures were characterized electrically by using Agilent B1500A Semiconductor Device Analyzer and GwInstec LCR-8110G Meter provided with a PSWI6 0-7.2 programmable power supply.

3. Results and Discussion

3.1 AFM results

Three-dimensional $5 \times 5 \mu\text{m}^2$ AFM surface images of 1000 nm thick non-irradiated homogeneous and composite a-Si-SiO_y films, as well as a 20 MeV electron irradiated with a fluence of $7.2 \times 10^{14} \text{ el} \times \text{cm}^{-2}$ homogeneous SiO_x film are depicted in figure 1. It is seen that the non-irradiated homogeneous layer (figure 1 (a)) has a relative rough, uniform surface with a root mean square (RMS) roughness of 2.38 nm, probably due to both low mobility of atoms because of the low substrate temperature (300 K) and the low kinetic energy of the evaporation process. The surface of the film annealed at 700°C for 30 min is significantly smoother (figure 1(b)) with RMS value of 1.3 nm, whereas the surface of the irradiated layer displays areas having very low roughness and areas with a slightly higher roughness; the RMS determined is 1.4 nm. Hence, similarly to the furnace annealing effect, the electron irradiation causes a surface roughness decrease. The surface of the composite sample irradiated with a flux of $7.2 \times 10^{14} \text{ el} \times \text{cm}^{-2}$ (not shown) also shows a fairly good smoothness but a few features are observed on the $5 \times 5 \mu\text{m}^2$ image with a height of ~ 40 nm and radius of the basis of 150 - 200 nm. The phase image of the surface with these features shows some phase lag, which may originate from different material properties. Excluding the features we obtained RMS value of 1.3 nm which equals to that of the non-irradiated composite films (annealed at 700 °C), which implies that the

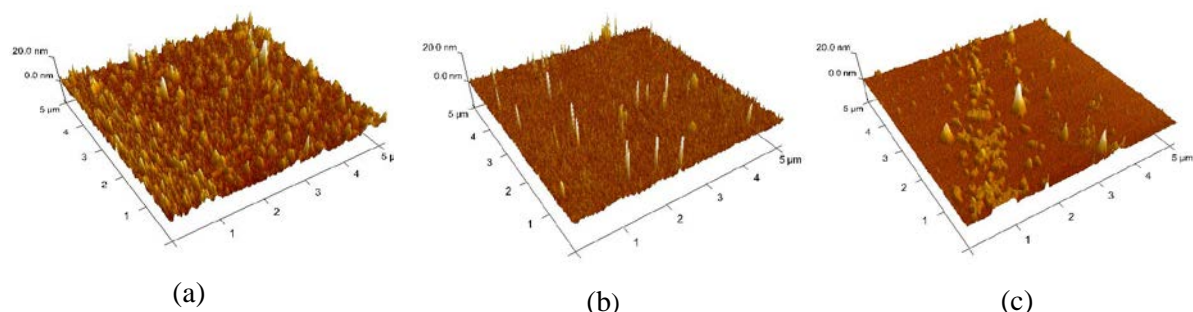


Figure 1. Three dimensional $5 \times 5 \mu\text{m}^2$ AFM surface images with 20 nm z-scale of structures with 1000 nm thick non-irradiated homogeneous SiO_x film (a), non-irradiated a-Si-SiO_y film (annealed at 700°C) (b) and 20 MeV electron irradiated homogeneous SiO_x film with a fluence of $7.2 \times 10^{14} \text{ el} \times \text{cm}^{-2}$ (c).

irradiation of the composite layers does not cause further smoothening of their surface. The phase images of the irradiated films have revealed quite large (hundreds of nanometers) regions of different phase. The changes in phase lag often indicate changes in the properties of the sample surface. The phase signal is sensitive to variations in composition, adhesion, friction, viscoelasticity etc., the understanding of the contribution of the individual factors to the phase shift observed is not simple.

A comparison of the described AFM results with our previous results on 20 MeV irradiated c-Si/SiO₂(20 nm thick) structures [9] shows some differences. The AFM images of the c-Si/SiO₂ (20 nm) structures irradiated with a fluence of $1.2 \times 10^{15} \text{ el} \times \text{cm}^{-2}$ and a beam current $I_e \approx 9 \text{ } \mu\text{A}$, have revealed a roughing of the surface accompanied by an increase in the crack density whereas an overall electron induced surface roughness decrease for c-Si/SiO_x structures has been observed in this study. The observed differences could be related to the 10 or 50 times greater thickness of the SiO_x layers and the approximately twice lower current ($I_e \approx 5 \text{ } \mu\text{A}$) used in this study. It seems that at electron beam current as low as 5 μA an annealing occurs, due to energy transfer from the electron beam to the film lattice, rather than defects formation causing a roughness increase.

3.2 Raman scattering results

Raman scattering spectra were collected on non-irradiated and irradiated c-Si/SiO_x and c-Si/(a-Si-SiO_y) structures with 200 and 1000 nm thick homogeneous or composite oxide films, as well as on the top and bottom surfaces of a bare c-Si substrate. The spectra of the non-irradiated and irradiated substrates were identical and indicate lack of Raman-detectable irradiation induced changes on the substrate surface. Moreover no appreciable irradiation induced changes in the c-Si-SiO_x structures with homogeneous SiO_x films have been detected.

Figure 2 shows Raman spectra of a non-irradiated c-Si/SiO_x and two 20 MeV electron irradiated c-Si/SiO_x(1000 nm) samples with fluences of $E_1 = 7.2 \times 10^{14} \text{ el} \times \text{cm}^{-2}$ and $E_2 = 1.44 \times 10^{15} \text{ el} \times \text{cm}^{-2}$. In all spectra the strong band situated at $\sim 521 \text{ cm}^{-1}$ is due to Raman scattering from 1TO phonons of the c-Si substrate. The low intensity feature at around 300 cm^{-1} is also due to light scattering from the c-Si substrate. The weak band at $\sim 430 \text{ cm}^{-1}$ is normally related [14] to scattering from amorphous SiO₂. The wide band located between 930 and 1030 cm^{-1} is assigned to multi-phonon scattering in the c-Si silicon substrate [15, 16]. Besides, no appreciable changes have been detected in 1000 nm films irradiated with a fluence of $2.4 \times 10^{14} \text{ el} \times \text{cm}^{-2}$ [10]. It is seen from figure 2 that the irradiation with three and six times higher fluences causes some changes in the Raman spectra. In order to make these changes clearer a linear baseline was subtracted from each spectrum in figure 2 and then the spectrum of non-irradiated sample was subtracted from the spectra of the irradiated ones. The result of this subtraction, i.e. the light scattering related to the irradiation induced changes in the films, is shown in the inset of figure 2. Two weak wide bands are seen at $\sim 150 \text{ cm}^{-1}$ and 480 cm^{-1} which are typical for a-Si [17]. Hence the 20 MeV electron irradiation with 7.2×10^{14} and $1.44 \times 10^{15} \text{ el} \times \text{cm}^{-2}$ causes appearance of amorphous silicon phase in the homogeneous SiO_x films, which resembles the results

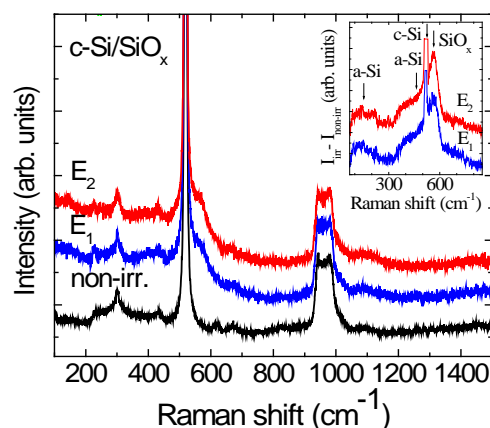


Figure 2. Raman spectra of a non-irradiated and two 20 MeV electron irradiated c-Si/SiO_x(1000 nm) samples with homogeneous SiO_x layers; irradiation fluences $E_1 = 7.2 \times 10^{14} \text{ el} \times \text{cm}^{-2}$, $E_2 = 1.44 \times 10^{15} \text{ el} \times \text{cm}^{-2}$. All spectra correspond to the same scale. The spectra of the irradiated samples practically coincide and the E_1 – spectrum is down shifted for clarity. Inset: curves obtained by subtracting the spectrum of the non-irradiated sample from the spectrum of the corresponding irradiated one.

reported in Ref.[9] though we detect amorphous silicon, not crystalline one. The formation of Si nanocrystals in the SiO_2 (20 nm) film upon 20 MeV electron irradiation observed in c-Si/ SiO_2 structures has been explained [9] assuming that the electron irradiation breaks the Si-O bonds, the free oxygen moves through the radiation defects and creates conditions whereby Si nanostructures are generated in the SiO_2 layer.

It can be also seen from figure 2 that a new band centered at $\sim 560 \text{ cm}^{-1}$ appears in the Raman spectra of the irradiated samples; its intensity is slightly higher in the spectrum of the sample irradiated with the higher fluence. No such band has been detected in the spectra of non-irradiated films. Such Raman scattering band has been observed in the spectra of SiO_x films prepared by thermal vacuum evaporation at similar deposition rates [18]. It has been related to specific light scattering from oxygen deficient SiO_x and considered as indication that the SiO_x films are build of combination of eight and six atom SiO rings with Raman active modes at 505 cm^{-1} and 606 cm^{-1} , respectively [19]. Due to low absorbance of the SiO_x , film thickness of $3 \mu\text{m}$ was necessary to observe the 560 cm^{-1} band [18]. As known SiO_x films prepared by thermal vacuum evaporation have a rather low density and the appearance of the 560 cm^{-1} band in the spectra of $1 \mu\text{m}$ thick films investigated here can be ascribed to an electron irradiation increase of the film density and/or increase of the amount of the eight and six atom SiO rings. It is possible that the phase changes observed in the AFM investigations are due to regions with an increased density and/or structural rearrangement.

Raman spectra of a non-irradiated and two 20 MeV electron irradiated c-Si/(a-Si- SiO_y (1000 nm)) samples with fluences of $E_1 = 7.2 \times 10^{14} \text{ el} \times \text{cm}^{-2}$ and $E_2 = 1.44 \times 10^{15} \text{ el} \times \text{cm}^{-2}$ are shown in figure 3. The bands of amorphous silicon at $\sim 150 \text{ cm}^{-1}$ and 480 cm^{-1} are well seen in the spectra of all composite films indicating existence of a quite large amount of amorphous silicon phase and their intensities are comparable. Moreover, the scattered light from all composite films is superimposed on a photoluminescence (PL) background, which is related to radiative recombination in the a-Si nanoparticles [12]. As seen from figure 3 the PL background in the spectra of the irradiated composite films is higher than that in the spectrum of non-irradiated film and it is higher for the greater irradiation fluence. Since the intensities of the a-Si bands are rather similar for all composite samples, these observations can be related to irradiation induced annealing of defects at the a-Si/ SiO_y interfaces and in the nanoparticle bulk rather than to an increase of the amorphous silicon phase. No photoluminescence background has been observed for the irradiated homogeneous films, which implies that either the amount of the a-Si phase or the nanoparticle size should be quite small.

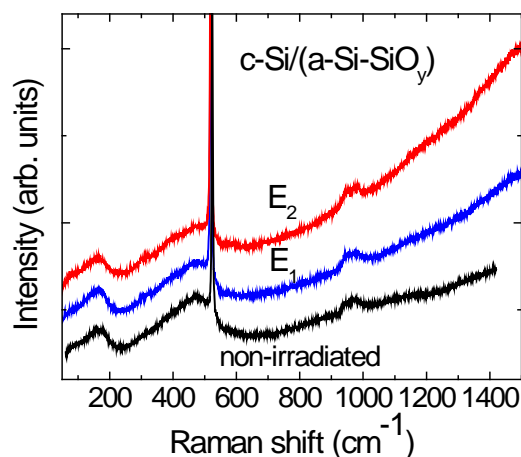


Figure 3. Raman spectra of a non-irradiated and two 20 MeV electron irradiated c-Si/(a-Si- SiO_y (1000 nm)) samples with fluences of $E_1 = 7.2 \times 10^{14} \text{ el} \times \text{cm}^{-2}$ and $E_2 = 1.44 \times 10^{15} \text{ el} \times \text{cm}^{-2}$. All spectra correspond to the same scale. The spectra of the irradiated samples practically coincide and the E_2 – spectrum is up-shifted for clarity.

3.3 Electrical characterization

The furnace annealing at 250°C for 30 min is not effective in reduction of the electrically active structural defects, the oxide layer thickness in the MOS structures is large and the C - V curves measured on both non-irradiated and irradiated samples with homogeneous SiO_x films have shown

rather complex behavior that requires further investigation. Therefore, here we will concentrate on the behavior of the structures with a-Si-SiO_y composite films, which experienced an annealing in argon for 60 min at 700°C. Figure 4(a) shows high frequency *C-V* hysteresis curves of non-irradiated and irradiated with a fluence of 1.44 e¹⁴cm⁻² n-MOS capacitors with 1000 nm thick composite oxide layer. The curves on the non-irradiated sample were measured in two voltage ranges: (+4 V to -3 V) and back (curve 1) and ± 40 V (curve 2). In order to avoid charging of the structures, the first measurement on each MOS capacitor investigated was carried out in a narrow enough range. In all measurements, scanning means that the gate bias was first swept from positive (accumulation regime) to negative (inversion regime) voltage and then in the reverse direction. Practically the curve 1 does not show hysteresis when compared to that of curve 2. The hysteresis of the ± 40 V scan is predominantly due to a shift of the *C-V* characteristic towards more negative voltages but a shift to more positive voltages is also seen (see also the positions of the maximums of the parallel conductance shown in figure 4(b), curves 2, measured simultaneously with the *C-V* curves in a single voltage scan. The shift to more negative voltages can be related to positive charging of both a-Si nanoparticles and traps in the SiO_y matrix, whereas the positive shift may be due to traps charged with electrons.

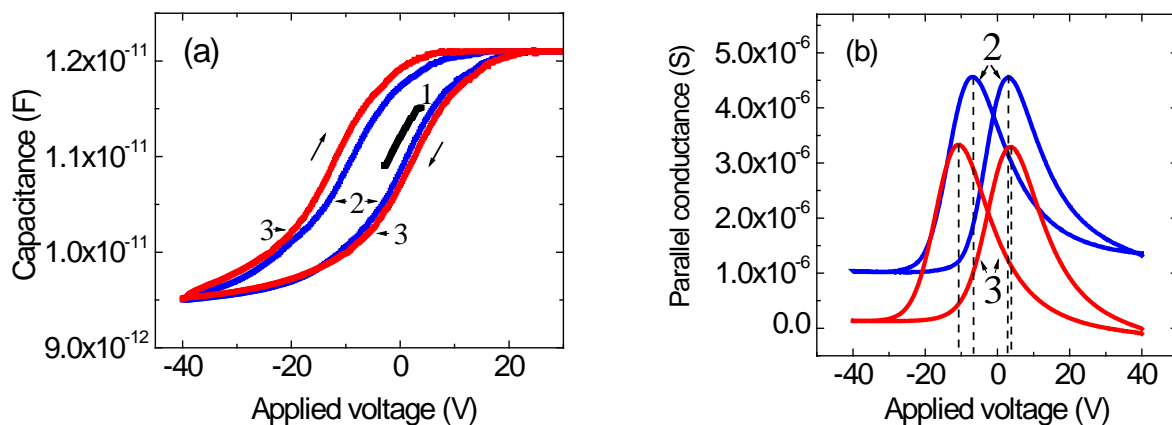


Figure 4. (a) *C-V* characteristics measured at 1 MHz of non-irradiated (curves 1, 2) and 20 MeV electron irradiated (curves 3) samples with 1000 nm thick composite a-Si-SiO_y layer, measured by sweeping the gate voltage in the (+3, -4 V) range, curve 1, and ± 40 V range, curves 2, 3; (b) Equivalent parallel conductance vs. gate bias measured simultaneously with the corresponding *C-V* characteristics.

A comparison of the *C-V* hysteresis curves of the irradiated n-MOS capacitor with 1000 nm thick composite oxide layer (figure 4, curves 3) with the curves of the non-irradiated one shows that there is no change of the capacitance value in accumulation. The result indicates that the electron irradiation did not cause appreciable changes of film thickness and dielectric constant. In addition, the curve slopes are quite similar which indicates that no significant increase of the interface traps occurred upon electron irradiation. However the electron irradiation causes an increase of the hysteresis and this increase is mainly due to a shift of the negative (left) branch of the *C-V* characteristic towards more negative voltages. This observation is supported by the parallel conductance results shown in figure 4(b) and can be related to an increase of either positive charge traps in the SiO_y matrix or the density of the a-Si nanoparticles. Since the Raman scattering results have not indicated an appreciable increase of the a-Si phase in the composite layers (Figure 3), one can infer that the electron irradiation of a-Si-SiO_y composite films causes an increase of the concentration of electrically active defects in the oxide matrix.

It is seen from figure 4(b) that the shape of the equivalent parallel conductance G vs. gate bias of both irradiated and non-irradiated samples is similar. The parallel conductance peak observed in the transition region between flatband conditions and weak inversion corresponds to energy loss due to carrier recombination through interface states [20]. If defects in the oxide layer contribute to the loss, they should be situated very close to the c-Si wafer/dielectric interface in order to be able to respond to the measuring frequency of 1 MHz. The similarity of the parallel conductance curves implies that the interface quality i.e. the defect density at the c-Si wafer/SiO_y interface of both samples is similar which is in agreement with the conclusion based on the similar slopes of the C - V curves (figure 4(a)).

As reported in Ref.[21] the 23 MeV electron irradiation of c-Si-SiO₂ (20 nm) MOS structures generates positive charges in the oxide and at the Si-SiO₂ interface. The former result is in good agreement with the assumed increase of positive charge traps in the SiO_y matrix of a-Si-SiO_y composite films whereas the latter is not confirmed by the initial results on c-Si/a-Si-SiO_y structures. This could be due to the fact that the suboxide layer deposited on the native oxide of the c-Si substrate somehow impedes interface defect creation but this point will be clarified in a future study.

4. Conclusions

Homogeneous, 200 nm and 1000 nm thick, SiO_x films ($x=1.3$) on crystalline (c-Si) substrate and composite a-Si-SiO_y films containing amorphous Si nanoparticles have been irradiated with 20 MeV electrons with two different fluences (7.2×10^{14} and 1.44×10^{15} el.cm⁻²). The amorphous Si nanoparticles were grown by an annealing of a part of the homogeneous SiO_x films in an argon atmosphere at 700 °C for 60 min. The AFM study of the effect of the electron irradiation on the surface morphology of both kinds of films have shown that the irradiation causes a significant decrease of the surface roughness of the homogeneous films, annealed at 250 °C, but no change in the surface roughness of the composite films, annealed at 700 °C, has been observed. These changes have been assigned to electron beam induced annealing. The Raman scattering data gave us basis to conclude that the electron irradiation causes formation of amorphous silicon phase in the homogeneous layers whereas in the composite layers it most likely improves the interface between the Si nanoparticles and the oxide matrix. The results from $C(G)$ - V measurements on irradiated MOS structures with composite films speak about formation of electrically active defects in the oxide matrix of the films.

Acknowledgements

This work is supported in the frames of Grant № 41/30.01.2013/p.17 from JINR, Dubna, Russia and Project INERA under the contract REGPOT 316309.

5. References

- [1] Fourches N T and Nenoï M 2012 *Current Topics in Ionizing Radiation Research* **32** 741 (Rijeka: InTech)
- [2] Oldham T R 2003 *IEEE Trans. Nucl. Sci.* **50** 483
- [3] Kaschieva S and Dmitriev S N 2010 *Radiation Defects in Ion Implanted and/of High-Energy Irradiated MOS Structures* (New York: Nova Science Publishers)
- [4] Krashennnikov A V and Nordlund K 2010 *J. Appl. Phys.* **107** 071301 and references therein
- [5] Takeguchi M, Tanaka M and K Furuya 1999 *Appl. Surf. Sci.* **146** 257
- [6] Chen G S, Boothroyd C B and Humphreys C J 1998 *Phil. Mag. A* **78** 491
- [7] Du X-w, Takeguchi M, Tanaka M and Furuya K 2003 *Appl. Phys. Lett.* **82** 1108
- [8] Kaschieva S, Gushterov A, Angelov Ch and Dmitriev S N 2012 *J. Phys.: Conf. Series* **356** 012005
- [9] Kaschieva S, Gushterov A, Angelov Ch and Dmitriev S N 2014 *J. Phys.: Conf. Series* **514** 012039
- [10] Nesheva D, Dzhurkov V, Scepanovic M, Bineva I, Manolov E, Kaschieva S, Nedev N, Dmitriev S N and Popovic Z V 2014 *J. Phys.: Conf. Series* **558** 012045

- [11] Nesheva D, Bineva I, Levi Z, Aneva Z, Merdzhanova T and Pivin J C 2003 *Vacuum* **68** 1
- [12] Nesheva D, Raptis C, Perakis A, Bineva I, Aneva Z, Levi Z, Alexandrova S and Hofmeister H 2002 *J. Appl. Phys.* **92** 4678
- [13] Donchev V, Nesheva D, Todorova D, Germanova K and Valcheva E 2012 *Thin Solid Films* **520** 2085
- [14] Rahmani A, Benoit M and Benoit C 2003 *Phys. Rev. B* **68** 184202
- [15] Temple P A and Hathaway C E 1973 *Phys. Rev. B* **7** 3685
- [16] Borowicz P, Latek M, Rzodkiewicz W, Łaszcz A, Czerwinski A and Ratajczak J 2012 *Adv. Nat. Sci.: Nanosci. Nanotechnol.* **3** 045003
- [17] Iqbal Z and Veprek S 1982 *J. Phys. C* **15** 377
- [18] Monticone E, Rossi A M, Rajteri M, Gonnelli R S, Lacquaniti V and Amato G 2000 *Phil. Mag. B* **80** 523
- [19] Pai P G, Chao S S, Takagi Y, Lucovski G 1986 *J. Vac. Sci. Technol. A* **4** 689
- [20] Nicollian E H, Brews J R 1982 *MOS Physics and Technology* (New York: Wiley–Interscience)
- [21] Kaschieva S, Halova E, Vlaikova E, Alexandrova S, Valcheva E and Dmitriev S 2006 *Plasma Processes and Polymers, Special Issue: Highlights from the 14th International Summer School on Vacuum, Electron and Ion Technologies* **3** 237